ANZIAM J. **62** (2020), 334–351
doi:10.1017/S1446181120000231

OPTIMAL LOCATION OF AN UNDERGROUND CONNECTOR USING DISCOUNTED STEINER TREE THEORY

K. G. SIRINANDA[1], M. BRAZIL[✉2], P. A. GROSSMAN[1], J. H. RUBINSTEIN[3] and D. A. THOMAS[1]

(Received 24 September, 2019; accepted 28 September, 2020; first published online 18 January, 2021)

Abstract

The objective of this paper is to demonstrate that the gradient-constrained discounted Steiner point algorithm (GCDSPA) described in an earlier paper by the authors is applicable to a class of real mine planning problems, by using the algorithm to design a part of the underground access in the Rubicon gold mine near Kalgoorlie in Western Australia. The algorithm is used to design a decline connecting two ore bodies so as to maximize the net present value (NPV) associated with the connector. The connector is to break out from the access infrastructure of one ore body and extend to the other ore body. There is a junction on the connector where it splits in two near the second ore body. The GCDSPA is used to obtain the optimal location of the junction and the corresponding NPV. The result demonstrates that the GCDSPA can be used to solve certain problems in mine planning for which currently available methods cannot provide optimal solutions.

2020 *Mathematics subject classification*: 90B80.

Keywords and phrases: network optimization, mine planning, underground mining, Steiner trees, net present value.

1. Introduction

The task of designing the decline access networks in underground mines in an optimal manner has been a challenge for the mining industry. In a typical mine planning scenario, the access network is designed with a view to minimizing the total development and infrastructure costs. A schedule for developing the access network and extracting the ore, optimally or otherwise, is constructed subsequently. It follows that the schedule

[1]Department of Mechanical Engineering, The University of Melbourne, VIC 3010, Australia; e-mail: kashyapa.sirinanda@gmail.com, peterag@unimelb.edu.au, doreen.thomas@unimelb.edu.au.
[2]Department of Electrical and Electronic Engineering, The University of Melbourne, VIC 3010, Australia; e-mail: brazil@unimelb.edu.au.
[3]Department of Mathematics and Statistics, The University of Melbourne, VIC 3010, Australia; e-mail: hyam.rubinstein@gmail.com.

and the time value of money cannot be taken into account when the access network is being designed. The recognition of the need for better techniques and algorithms for this stage of mine planning is the driving force in the investigation described in this paper. Specifically, we describe a case study which demonstrates that a mine planning algorithm developed by the authors, and described in an earlier paper, can be used in real mine planning problems.

In the remainder of this section we present some basic mining background relevant to the present problem, introduce net present value as a measure of the time value of money, discuss methods which have been developed previously for generating optimal mine designs, and introduce the concepts needed for the algorithm used in the case study.

We begin with an introduction to mining, focusing on the concepts that are relevant to the present paper. Mines can be classified as open pit mines, underground mines or a combination of both. Open pit mines are generally used when the resources are near to the earth's surface, while underground mines are used when the resources are deeper. Extraction in underground mines typically occurs on a number of levels, and access to the levels from the surface can be provided by shafts or declines. A decline is a tunnel that slopes downward into the mine. In a complex mine with several ore bodies there will typically be a network of declines. The decline network is used by the vehicles that transport personnel and equipment into the mine and by the trucks that carry the ore and waste rock to the surface. There are two main items of equipment used both to construct the decline network and to extract the ore. *Jumbos* are vehicles with one or more booms which are used to drill into the rock face prior to setting explosives. *Load-haul-dump vehicles* have a scoop which is used to transport broken rock from the development face to ore trucks or underground stockpiles.

Next, we introduce the concept of net present value. Consider a series of cash flows: incoming or outgoing payments that occur at specified times. The potential for currently held cash to generate value by being invested is accounted for by discounting each future cash flow to the present time, using a discount rate which is typically expressed as a percentage per annum. The algebraic sum of the discounted cash flows (treating incoming payments as positive and outgoing payments as negative) is known as the *net present value* (NPV) of the cash flow series. The NPV reflects the time value of money by measuring the present value of a future investment. It is assumed that the discount rate does not vary over the time period under consideration.

We now discuss the process of designing a mine using optimization methods, where the NPV of the mine is the objective to be maximized. The current methods for designing open pit mines are reliable, accurate and relatively simple [7, 10, 25]. In recent decades, there have been major developments towards methods that maximize the NPV of open pit mines. By contrast, mathematical models to maximize the NPV for underground mines that take into account the construction of the access network have not been developed. Existing methods for designing underground mines do not generally use optimization techniques.

https://doi.org/10.1017/S1446181120000231 Published online by Cambridge University Press

The mining industry started to use optimization techniques in the late 1960s, and they were initially used for the production scheduling of open pit mines [12, 14]. In recent years, these results and some other ideas relating to open pit mines have been used to implement mathematical models for optimizing underground mines or a combination of open pit and underground operations. Ben-Awuah et al. [1] used mixed integer linear programming to investigate mining strategies for maximizing NPV, when the options of open pit, underground, and concurrent open pit and underground mining are available. King and Newman [11] developed a mixed integer programming (MIP) algorithm for optimizing the cut-off grades in pre-determined zones in an underground mine for maximum NPV. Little et al. [13] developed and applied an MIP model that simultaneously optimizes the layouts of the stopes (minable blocks of ore) and the production schedules for maximum NPV. Grossman et al. [8] developed and applied an exact algorithm for scheduling the construction of an underground mine for maximum NPV, where the design of the access network is given and one face can be worked at any given time. Recently, Hou et al. [9] developed an integrated model for the simultaneous optimization of designing the stopes and the access layout in underground mines using mixed integer nonlinear programming, with undiscounted value as the objective. However, most of the techniques for maximizing the NPV of underground mines have been applied only to specific mines [15, 16, 24], and limited underlying theory has been developed that can be applied more generally.

We now investigate the design of decline access networks in more detail. At this point the reader may find it helpful to look ahead to Figures 1 and 2 in Section 2, which show the layout of the mine used in the case study and a simple representation of part of the decline network, respectively. We assume that the locations of the surface portal and the points where each level is to be accessed are given, and the access network must connect these points. The ramp gradient must be within a safe and economic climbing limit for trucks, typically in the range of 1 : 9 to 1 : 7. A minimum turning radius for curved ramps determined by trucks and other equipment is typically in the range of 15 to 40 metres. Further constraints may be imposed by the ground conditions and other geotechnical factors. The underground access network needs to be optimized both topologically and geometrically subject to the gradient, curvature and any other constraints.

Junction points occur in the network where three ramp segments meet. In the model of the network these points are represented by variable nodes, because their optimal location depends on the objective function. If the objective is to minimize the total length of the ramp segments and the gradient and curvature constraints are disregarded, then the problem is an instance of the well-known Steiner tree problem. The junction points are known as Steiner points, and if the lengths of the ramp segments are given by the standard Euclidean metric, then the locations of the Steiner points can be determined using the well-established theory of Euclidean Steiner networks [6]. In underground mines, however, the junctions must be placed to avoid violating the gradient [3, 5] and curvature constraints [2]. The optimization problem becomes more complicated, even for a network with a single junction point, when subjected

https://doi.org/10.1017/S1446181120000231 Published online by Cambridge University Press

to these constraints. Optimizing the model for maximum NPV introduces additional complications, since the optimal location of a Steiner point depends on the time taken for the decline development to reach its location and on the order of reaching the points where the ore is extracted, and these in turn depend on the value of the mined material.

Brazil et al. [3] and Brazil and Thomas [4] studied underground mine access design processes and described how to locate the Steiner points. The objective of the problem they analysed was to minimize the infrastructure and haulage costs of an underground mine. However, they did not take the discounted cost into account in their model, and they did not study the problem of locating the Steiner point with the objective of maximizing the NPV. In what follows, we refer to such points as *discounted Steiner points*.

The underground mine access construction process can be classified according to the availability of the mining equipment. The 1-Face and 2-Face discounted Steiner point algorithms described in the literature [18, 19, 23] can be used to optimally locate a single discounted Steiner point for maximum NPV, given the locations of the three adjacent points, when the mine is being developed with one and two concurrent development faces, respectively, with no gradient or curvature constraints on the declines. The authors emphasized that the time value of money has a crucial effect on locating the junction points in the access network for maximum NPV. The algorithm discussed by Sirinanda et al. [18] locates a junction point to access ore bodies most efficiently in the absence of gradient and curvature constraints, thus maximizing the NPV in that case. The authors showed that in the maximum NPV network joining three points, the paths from the junction point to the breakout point and the first resource point make equal angles with the path from the junction point to the second resource point. The algorithm provides higher NPV compared with the placement of the junction point at the location where the development length is minimized.

We now introduce the gradient constraint into the model. We represent the underground access network as a tree, where the locations of the ore resource points and the root (corresponding to the surface portal or a breakout from an existing decline) are given, and the junction points of the network are to be obtained for a given objective function. An edge in the tree is labelled as a b edge, an m edge, or an f edge if the gradient between its endpoints is greater than, equal to, or less than the maximum gradient, respectively [21]. The *labelling* of a discounted Steiner point is a list of the three incident edge labels taken in the order in which the edges are constructed, with a chevron placed over a label if the corresponding edge lies above the discounted Steiner point. For example, $\hat{f}\hat{m}b$ is the labelling for a discounted Steiner point s where the first edge to be constructed is an f edge above s, the second edge is an m edge above s, and the third edge is a b edge below s. Sirinanda et al. [22] showed that only some of the potential labellings are actually feasible. The gradient-constrained discounted Steiner point algorithm (GCDSPA) [22] determines the optimal location of a discounted Steiner point in the presence of an upper bound on the gradient in a network by investigating all feasible labellings of the point.

https://doi.org/10.1017/S1446181120000231 Published online by Cambridge University Press

The objective of this paper is to demonstrate the applicability of the GCDSPA to real mine planning problems by conducting a case study. The GCDSPA is used to design a connector between the access networks associated with two ore bodies. The ore bodies used in this study are Rubicon and Hornet, which occur in the Rubicon gold mine in the Kundana mining region near Kalgoorlie, Western Australia. The aim is to design an underground connector between Rubicon and Hornet so as to maximize the NPV associated with that connector. The connector will break out from the access infrastructure of Rubicon and extend to Hornet. The connector will split into two at a junction point near the Hornet end, and the GCDSPA developed by Sirinanda et al. [22] is used to obtain the optimal location of the junction point and the corresponding NPV.

The case study is described in Section 2 and the GCDSPA is described in Section 3. In Section 4 the given data are prepared so that the GCDSPA can be applied. The results are discussed in Section 5. Section 6 contains some concluding remarks, including a proposal for future research.

2. Case study: designing the Rubicon–Hornet connector

2.1. General aim of the case study In this section we describe the case study in which we use the GCDSPA to design the optimal connector between two ore bodies, Rubicon and Hornet, in the Rubicon gold mine. The motivation behind the investigation is to validate and test the effectiveness of the GCDSPA by applying it to a typical mining operation. In doing so, the case study should provide insight into the benefits of the new approach.

The Rubicon ore body is located beneath a previously mined open pit. Access to the Rubicon ore body is via an existing decline. The Hornet ore body is located 600 m to the south of the Rubicon ore body. Access to the Hornet ore body is to be via a decline (or connector) developed off the Rubicon decline. The connector will join a decline that provides access to the Hornet ore body. Ore is to be extracted from each level of Hornet through a drawpoint located on the Hornet decline at that level. The layout of the Rubicon and Hornet ore bodies and their grade distributions (gold content in grams per tonne), and the existing and proposed access network, are shown in Figure 1 [17]. One jumbo and associated equipment are available to construct the connector.

The aim of the investigation is to design an underground connector between Rubicon and Hornet so as to maximize the NPV associated with the connector as shown in Figure 2. The connector is to break out from the existing access infrastructure at Rubicon and extend to Hornet.

2.2. Inputs The algorithm requires the following inputs.

- The coordinates of a set of potential breakout points on the existing Rubicon access.

https://doi.org/10.1017/S1446181120000231 Published online by Cambridge University Press

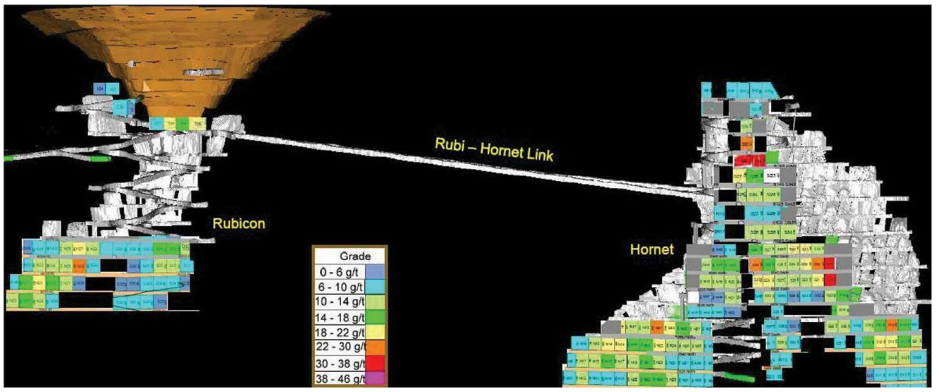

FIGURE 1. Layout of the Rubicon and Hornet ore bodies and access network. (Colour available online.)

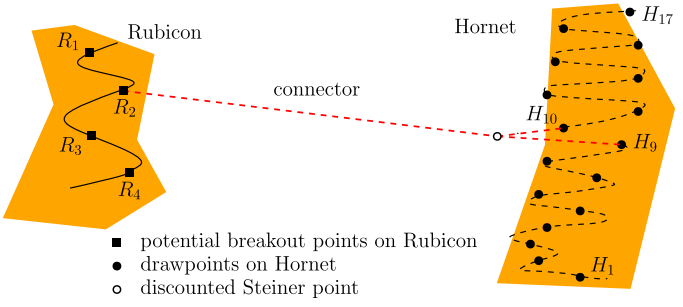

FIGURE 2. The Rubicon and Hornet connector.

- A set of drawpoints at Hornet, one drawpoint for each level. For each drawpoint, the coordinates of the point, the tonnage of ore to be extracted from that level and the average grade of the ore on the level are required.
- Other parameters, namely, the cost per metre of constructing tunnels, the rate of tunnel construction, the maximum decline gradient, the discount rate for the NPV calculation, the market price of gold and the cost per tonne of extracting and processing the ore.

2.3. Assumptions The following assumptions are made.

- The connector breaks out from one of the given set of breakout points on Rubicon and connects to two adjacent drawpoints on Hornet via a single junction which corresponds to a discounted Steiner point [22]. All possible pairs of adjacent drawpoints in Hornet are to be considered in the optimization.
- Access to the other drawpoints on Hornet is via maximum gradient declines up or down from the drawpoints associated with the connector.
- The mine is being operated with a single development face at any given time. This assumption is reasonable, since the jumbo continues to develop the access

https://doi.org/10.1017/S1446181120000231 Published online by Cambridge University Press

TABLE 1. The potential breakout points on the Rubicon access, with coordinates (in metres) x, y, z.

Rubicon breakout point	x	y	z
R_1	9833.374	16 185.869	6208.288
R_2	9839.279	16 179.883	6162.217
R_3	9831.543	16 185.044	6120.056
R_4	9824.143	16 174.721	6078.452

in Rubicon at the same time as it is building the connector and so it is not at risk of being idle.
- The curvature constraint on declines is ignored. Again this assumption is reasonable, given that the distances involved in the connector are large compared to the turning radius.
- For each pair of adjacent drawpoints, the drawpoint with the higher aggregated value is extracted first, where aggregated value is defined in Section 4.3.
- The input parameters are deterministic and time-independent.

2.4. Anticipated outputs from the case study The anticipated outputs are:

- the optimal design of the connector, defined by the location of the junction and the choice of the breakout point and the two drawpoints;
- the optimal NPV associated with this design.

2.5. Data The data for the case study were supplied by Rand Mining Limited and Tribune Resources Limited. The data values used are approximations to the true values, but they are sufficiently accurate to provide a demonstration of the applicability of the approach in practice using realistic data at realistic problem scales.

- Development cost rate: \$5000/m
- Development rate: 140 m/month with a single heading
- Maximum decline gradient: 1 : 7
- Discount rate: 10% p.a.
- Market price of gold: \$800/oz t = \$25.7205973/g
- Milling, administration and maintenance costs: \$27.35/tonne

The maintenance costs comprise underground road maintenance costs, the fixed plant cost, and power and water supply costs.

The coordinates of the Rubicon breakout points are given in Table 1. Details of the Hornet drawpoints are in Table 2 (in the Appendix). The x, y, z coordinates in the tables are in metres with respect to an arbitrary origin.

3. The gradient-constrained discounted Steiner point algorithm

In this section we provide an outline of the GCDSPA algorithm. Further details may be found in [22].

https://doi.org/10.1017/S1446181120000231 Published online by Cambridge University Press

The inputs to the GCDSPA are:

- the coordinates of the three points p_0, p_1 and p_2 adjacent to the discounted Steiner point. It is assumed that the decline from p_0 to p_1 via the discounted Steiner point is to be constructed first, followed by the decline from the discounted Steiner point to p_2;
- the net values at p_1 and p_2, respectively;
- the cost rate of developing the declines in dollars per metre;
- the rate of developing the declines in metres per year;
- the discount rate as a percentage per annum;
- the maximum decline gradient.

The outputs are the optimal location of the discounted Steiner point, the optimal labelling and the corresponding value of the NPV.

The algorithm proceeds by calculating the optimal solution for each of four cases and then determining which of these solutions is the globally optimal solution. Recall from Section 1 that each edge has a label (b, m or f) depending on its gradient, and each discounted Steiner point has a labelling based on the labels of the three edges incident to it. For each case a number of different labellings must be explored because the formulae for computing lengths in the network depend on the labelling. However, according to the theory developed in by Sirinanda et al. [22], only certain labellings can occur in each case and so it is not necessary to explore all possible labellings. They provide [22, Theorems 1–7] the means for determining the location of a discounted Steiner point for all labellings that can occur. For each labelling, the solution is obtained by solving a certain system of equations simultaneously.

CASE 1. The optimal solution has three edges, including at least two m edges. The discounted Steiner point is determined using Theorems 1, 2 and 3 of [22], which deal with labellings comprising three m edges, two m edges and one b edge, and two m edges and one f edge, respectively. The corresponding NPV is calculated and the labelling is recorded.

CASE 2. The optimal solution has three edges, including exactly one m edge. The discounted Steiner point is determined using Theorems 4 and 5 of [22], which deal with labellings comprising one edge of each label, and two f edges and one m edge, respectively. The corresponding NPV is calculated and the labelling is recorded.

CASE 3. The optimal solution has three edges, none of which are m edges. The discounted Steiner point is determined using Theorems 6 and 7 of [22], which deal with labellings comprising three f edges, and two f edges and one b edge, respectively. The corresponding NPV is calculated and the labelling is recorded.

CASE 4. The optimal solution has only two edges, that is, the discounted Steiner point is located at p_1 or p_2. The discounted Steiner point is determined, the corresponding NPV is calculated and the labelling is recorded.

https://doi.org/10.1017/S1446181120000231 Published online by Cambridge University Press

In the final step, the case that delivers the maximum NPV is determined and the corresponding discounted Steiner point location and labelling are output.

4. Pre-processing of the data

In this section the given data are pre-processed so that they can be used as input for GCDSPA.

4.1. Calculation of the net gold values The net gold value at each level of Hornet is calculated from the tonnage and average grade at the level given in Table 2, the market price of gold per gram and the costs per tonne of ore. The results are shown in the final column of Table 2.

The costs of extracting the ore and hauling it to the surface were not included when calculating the net gold values because the data needed to determine them were not provided by the mining company. From the point of view of finding the optimal design for the connector, ignoring these costs is equivalent to treating them as constants with no time discounting.

4.2. Enumeration of cases The data are organized such that GCDSPA can be applied. There are 16 cases, corresponding to the 16 pairs of adjacent Hornet drawpoints. In what follows, the cases are numbered starting from the lowest pair of levels of the Hornet ore body. For each of these cases, four Rubicon breakout points are considered, which yields 64 subcases altogether. For each subcase, the discounted Steiner point could be either above or below the adjacent breakout point and either above or below each of the adjacent drawpoints.

4.3. Calculating aggregated values In order to be able to apply the GCDSPA, quantities known as aggregated values need to be calculated. The aggregated value at a point is the sum of the values at the nodes in the network beyond the point minus the construction costs of the associated access, with appropriate discounting applied.

Let d be the discount rate per annum, let C be the decline construction cost per metre, and let D be the decline development rate in metres per year. Consider a point p where we want to calculate the aggregated value. Let $r = 1 + d$ and $V_c = CD/\ln r$. A point with value V at a distance l from p along the decline contributes $Vr^{-l/D}$ to the aggregated value. If a decline of length l is to be constructed then the discounted construction cost is

$$\int_0^l Cr^{-x/D}dx = V_c r^{-l/D} - V_c,$$

and this quantity is subtracted from the total of the discounted values of the points to obtain the aggregated value at p.

The net values in each level of Hornet are used to calculate aggregated values for the two adjacent drawpoints. The Hornet drawpoints $H_1, H_2, \ldots, H_{17}$ have net values $V_1, V_2, \ldots, V_{17}$, respectively. The process for calculating the value aggregations can be described by considering Case 9, as shown in Figure 3. The aggregated value is cal-

https://doi.org/10.1017/S1446181120000231 Published online by Cambridge University Press

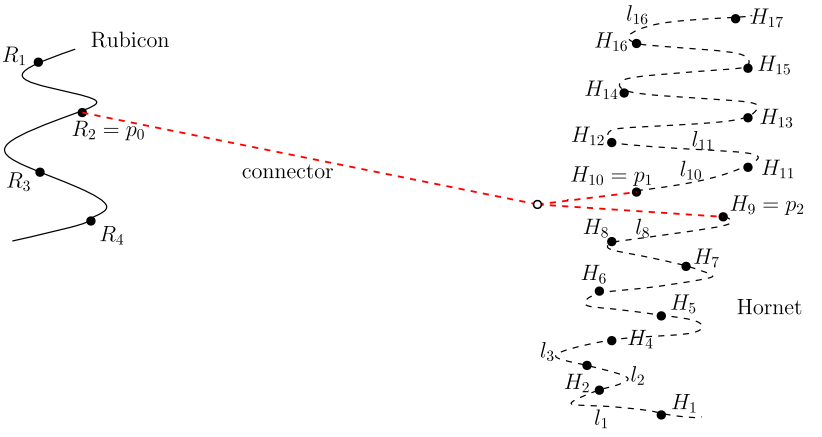

FIGURE 3. Access network design for Case 9. As in Figure 2, the discounted Steiner point is indicated by an open circle.

culated by discounting the ore production and access construction costs of the Hornet decline to the corresponding aggregated point. The net values at the points $H_{10}, \ldots, H_{17}$ are aggregated to the point H_{10} and the net values at the points $H_1, H_2, \ldots, H_9$ are aggregated to the point H_9. All the values of the points below H_9 are discounted at the aggregated point H_9. Similarly, all the values of the points above H_{10} are discounted at H_{10}. It is assumed that the points $H_1, H_2, \ldots, H_8$ are connected to the point H_9 by a single decline with the maximum gradient. Similarly, the points $H_{11}, \ldots, H_{17}$ are connected to the point H_{10} by a single decline with the maximum gradient.

Let $l_i = \left|z_{H_{i+1}} - z_{H_i}\right| \sqrt{1 + m^{-2}}$ be the distance from the point H_i to H_{i+1} measured by the gradient metric, where m is the maximum gradient and z_{H_i} is the z-coordinate of the ith Hornet drawpoint. Let $t_i = l_i/D$ be the time taken to construct the decline link from H_i to H_{i+1}. The aggregated value at the point H_{10} is $\bar{V}_x$, which can be expressed as

$$\begin{aligned}\bar{V}_x = {} & V_{10} + V_{11} r^{-l_{10}/D} + V_{12} r^{-(l_{10}+l_{11})/D} + V_{13} r^{-\sum_{i=10}^{12} l_i/D} + V_{14} r^{-\sum_{i=10}^{13} l_i/D} \\ & + V_{15} r^{-\sum_{i=10}^{14} l_i/D} + V_{16} r^{-\sum_{i=10}^{15} l_i/D} + (V_{17} + V_c) r^{-\sum_{i=10}^{16} l_i/D} - V_c. \end{aligned} \tag{4.1}$$

The aggregated value at the point H_9 is $\bar{V}_y$, which can be expressed as

$$\begin{aligned}\bar{V}_y = {} & V_9 + V_8 r^{-l_8/D} + V_7 r^{-(l_8+l_7)/D} + V_6 r^{-\sum_{i=6}^{8} l_i/D} + V_5 r^{-\sum_{i=5}^{8} l_i/D} \\ & + V_4 r^{-\sum_{i=4}^{8} l_i/D} + V_3 r^{-\sum_{i=3}^{8} l_i/D} + V_2 r^{-\sum_{i=2}^{8} l_i/D} + (V_1 + V_c) r^{-\sum_{i=1}^{8} l_i/D} - V_c. \end{aligned} \tag{4.2}$$

This same procedure is followed when calculating the aggregated values for the other cases as shown in Table 3 (in the Appendix).

5. Results

In the trial, each pair of adjacent Hornet drawpoints p_1 and p_2 was considered with each breakout point p_0 of Rubicon, which yielded 64 subcases in total. The GCDSPA

https://doi.org/10.1017/S1446181120000231 Published online by Cambridge University Press

was applied in these subcases and the optimal labellings, the optimal location of the junction point and the corresponding NPV were obtained as shown in Tables 4–7 (in the Appendix). Recall that a chevron placed over b, m or f in a labelling denotes that the corresponding edge lies above the horizontal plane containing the junction point.

The gradients corresponding to the labellings are also shown in the tables. The gradients g_1, g_2, g_3 are measured between the junction point and the adjacent points p_0, p_1, p_2, respectively. Note that for the case of a b edge the actual gradient of the corresponding decline would be the maximum permitted gradient and not the gradient in the table.

Here, an edge is labelled $x_1x_2x_3$, where

$$x_i = \begin{cases} b & \text{when } g_i > 0.1429, \\ m & \text{when } g_i = 0.1429, \\ f & \text{when } g_i < 0.1429, \end{cases}$$

for each $i = 1, 2, 3$.

5.1. Breakout point at R_1 In the scenario where the breakout point is at R_1, the optimal locations of the junction point were obtained for 15 of the 16 cases listed in Table 3. The points p_0 (R_1) and p_1 are above the point p_2 for Cases 1–7. Therefore, the labellings $\hat{m}\hat{m}m$, $\hat{m}\hat{m}b$, $\hat{m}\hat{f}b$, $\hat{m}\hat{f}m$, $\hat{f}\hat{m}b$, $\hat{f}\hat{m}m$, $\hat{f}\hat{m}f$, $\hat{f}\hat{f}b$, $\hat{f}\hat{f}m$, $\hat{f}\hat{f}f$ need to be considered in these cases [21]. The points p_0 (R_1) and p_2 are above the point p_1 for Cases 8–14, therefore, the labellings $\hat{m}b\hat{m}$, $\hat{m}m\hat{m}$, $\hat{m}m\hat{f}$, $\hat{f}m\hat{m}$, $\hat{f}m\hat{f}$, $\hat{f}f\hat{m}$, $\hat{f}f\hat{f}$ need to be considered in these cases [21]. The point p_2 is above the points p_0 (R_1) and p_1 for Case 15.

As shown in Table 4, the optimal solution is given by Case 10 and the optimal labelling is $\hat{m}b\hat{m}$ with the maximum NPV of \$82 973 572. For Cases 12–15 the optimal location of the junction point is p_2, which corresponds to a degenerate case of the discounted Steiner point. In the optimal configuration for these cases, p_0 and p_2 are connected by a straight line corresponding to an f edge, and p_2 and p_1 are connected by a zigzag line corresponding to a b edge.

Case 16 in Table 3 is not considered for two reasons. First, the Rubicon breakout point is below the Hornet drawpoints and so the solution would have downward haulage which is unlikely to be optimal. Second, as seen in the last column of Table 4, the optimal NPV increases up to Case 10 and decreases thereafter. Hence it is reasonable to disregard the last case.

5.2. Breakout point at R_2 Table 5 shows the optimal locations of the junction point, the optimal labellings and corresponding NPVs for Cases 1–12 of the 16 cases listed in Table 3, when the breakout point is at R_2. The other four cases from Table 3 are not applicable as the breakout point is below the two drawpoints as before. The optimal configuration when the breakout point is at R_2 occurs with Case 7, with labelling $\hat{m}\hat{m}b$ and corresponding maximum NPV of \$ 83 478 168.

https://doi.org/10.1017/S1446181120000231 Published online by Cambridge University Press

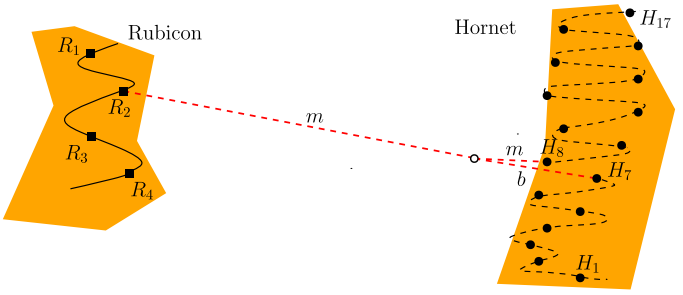

FIGURE 4. Optimal solution for the case study. The legends for this figure are the same as in Figure 2.

5.3. Breakout point at R_3 In this case the breakout point is fixed at R_3 and the optimal locations of the junction, the optimal labellings and the corresponding NPVs were obtained for ten cases from Table 3. As before, the other six cases are not applicable as the Hornet drawpoints are above the Rubicon breakout point. Table 6 shows the variation of the junction point for the optimal labellings. When the breakout point is at R_3, Case 6 provides the optimal configuration with the maximum NPV of \$ 83 324 417.

5.4. Breakout point at R_4 Table 7 shows the optimal locations of the junction point, the optimal labellings and the corresponding NPVs for eight cases. Again, the other cases are not applicable as explained above. Case 4 provides the optimal location of the junction, the optimal labelling $\hat{m}\hat{m}b$ and the corresponding maximum NPV of \$ 82 979 145.

5.5. Globally optimal solution Table 8 (in the Appendix) shows the optimal labelling and corresponding NPV when the breakout points are at R_1, R_2, R_3 and R_4. The maximum NPV taken over all breakout points is \$ 83 478 168, and it occurs when the connector starts from Rubicon breakout point R_2 and connects to the Hornet drawpoints H_7 and H_8. The optimal labelling is $\hat{m}\hat{m}b$ and the optimal location of the junction is (9842.118, 15 508.049, 6066.239).

The results show that the connector joins at the highest-grade ore locations which are situated at H_7 and H_8 in Hornet, as shown in Figure 4. This outcome is not unexpected, given that a high value for NPV is typically achieved by accessing high-value ore as early as possible.

The computations were performed on an Intel® Core™ i7-2600 CPU at 3.40 GHz with 3.23 GB RAM. Each of the 64 subcases took less than 1 minute to run.

6. Conclusion

The GCDSPA was successfully applied to the Rubicon and Hornet ore bodies in the Kundana group of mines in Western Australia. An underground connector was

https://doi.org/10.1017/S1446181120000231 Published online by Cambridge University Press

designed between Rubicon and Hornet so as to maximize the NPV associated with the connector. The connector breaks out from the access infrastructure of Rubicon and connects via a junction to two locations at Hornet. The GCDSPA was used to obtain the optimal location of the junction point on the connector and the corresponding NPV. The optimal location given by the algorithm is (9842, 15 508, 6066) which yields an NPV of $ 83.5 million.

This study has demonstrated the applicability of the GCDSPA to solving a class of NPV maximization problems in mine planning by using a realistic representative scenario. Further, we believe that our study is the first application of an optimization algorithm to designing an underground mine access network for maximum NPV. Currently, access network design is carried out manually by a mine design engineer without using any formal optimization process, or by using software that optimizes for minimum cost. Optimization for maximum NPV has previously been applied to other aspects of underground mine design, typically using MIP. However, the geometric optimization method used in the present study is more appropriate here, due to the inherently continuous nature of the problem as opposed to the discrete problems to which MIP methods are well suited.

The situation at the mine changed after the data had been provided to the researchers. The design that was ultimately used for the connector broke out from the Rubicon decline near R_1 and connected to the Hornet decline near H_{15}. That design was chosen because a second jumbo had become available, and so it was advantageous to reach the Hornet decline early to allow both jumbos to be fully utilized. The algorithm used in this case study could not have obtained that solution, because it does not take the availability of multiple items of equipment into account. A fruitful topic for future research would be to extend the model to enable it to handle such scenarios. This could be achieved by modifying the 2-Face discounted Steiner point algorithm described by Sirinanda et al. [23] to take account of the constraint on the gradient, by considering all the feasible labellings of the Steiner point in a similar manner to the approach used in the present study.

The algorithm used in the present study can be applied only to networks containing a single discounted Steiner point. In practice, the access networks in underground mines contain many junctions. Sirinanda et al. [20] derived an algorithm for networks with two discounted Steiner points and no gradient constraint. In the light of the successful outcome of the present study, we propose that extending the algorithm to handle networks with multiple junctions would be a worthwhile area of future research with potentially substantial benefits for the mining industry.

Another area for investigation is to explore the sensitivity of the outputs of the algorithm to variations in the discount rate and other parameters such as the gold price. By running the model with a variety of values for the parameters, ranges of parameter values could be established for which the optimal location of the connector does not change. The model could also be extended to a stochastic model to account explicitly for the uncertainty in the parameters.

https://doi.org/10.1017/S1446181120000231 Published online by Cambridge University Press

Appendix: Tables

TABLE 2. The drawpoints for the Hornet access, one for each level, with coordinates (in metres) x, y, z.

Hornet	x	y	z	Tonnes	Av. grade (g/t Au)	Net value ($)
H_1	9820.620	15 517.796	5921.472	44 465	4.96	4 456 467
H_2	9818.091	15 528.853	5943.130	41 381	7.05	6 371 855
H_3	9840.623	15 531.109	5962.314	38 579	7.39	6 277 776
H_4	9832.170	15 525.640	5983.492	42 745	8.33	7 989 151
H_5	9838.951	15 516.830	6002.379	41 152	8.57	7 945 444
H_6	9834.968	15 528.034	6023.395	32 099	10.34	7 658 853
H_7	9842.123	15 511.853	6042.983	34 868	11.05	8 956 285
H_8	9838.533	15 525.413	6063.707	38 983	11.39	10 354 181
H_9	9841.863	15 504.792	6083.575	36 973	9.40	7 927 884
H_{10}	9840.487	15 521.042	6104.712	35 223	8.12	6 393 019
H_{11}	9846.451	15 501.936	6123.909	32 037	8.64	6 243 241
H_{12}	9850.112	15 527.268	6144.418	28 732	7.65	4 867 562
H_{13}	9853.493	15 501.562	6164.579	24 569	10.44	5 925 380
H_{14}	9857.259	15 525.142	6184.610	18 415	10.09	4 275 426
H_{15}	9863.145	15 500.162	6204.046	17 559	7.36	2 843 743
H_{16}	9861.849	15 521.812	6224.877	15 460	7.17	2 428 251
H_{17}	9878.129	15 504.200	6243.582	28 594	4.34	2 409 828

TABLE 3. Aggregated values at the Hornet drawpoints for each case.

Case	First Hornet drawpoint	Second Hornet drawpoint	First aggregated value	Second aggregated value
1	H_2	H_1	84 143 041	4 456 467
2	H_3	H_2	78 959 226	10 027 362
3	H_4	H_3	74 053 506	15 552 612
4	H_5	H_4	67 237 096	22 664 608
5	H_6	H_5	60 539 806	29 773 745
6	H_7	H_6	53 993 391	36 442 735
7	H_8	H_7	46 148 845	44 423 953
8	H_8	H_9	53 680 676	36 786 340
9	H_9	H_{10}	60 482 767	29 854 678
10	H_{10}	H_{11}	65 620 957	24 324 373
11	H_{11}	H_{12}	70 684 681	18 958 598
12	H_{12}	H_{13}	74 250 954	14 921 152
13	H_{13}	H_{14}	78 868 310	9 779 405
14	H_{14}	H_{15}	81 807 157	6 256 818
15	H_{15}	H_{16}	83 331 043	4 161 217
16	H_{16}	H_{17}	84 380 955	2 409 828

https://doi.org/10.1017/S1446181120000231 Published online by Cambridge University Press

TABLE 4. Optimal labellings and the optimal location of the junction when the breakout point is at R_1.

Case	Optimal labelling	Optimal location of the junction			Gradients			Optimal NPV $
		x	y	z	g_1	g_2	g_3	
1	$\hat{m}\hat{m}b$	9806.935	14 929.498	6028.766	0.1429	0.1429	0.1823	67 988 128
2	$\hat{m}\hat{m}b$	9823.971	14 997.728	6038.548	0.1429	0.1429	0.1796	69 662 337
3	$\hat{m}\hat{m}b$	9839.780	15 069.009	6048.734	0.1429	0.1429	0.1870	71 785 782
4	$\hat{m}\hat{m}b$	9835.462	15 130.676	6057.545	0.1429	0.1429	0.1874	73 487 203
5	$\hat{m}\hat{m}b$	9839.694	15 209.853	6068.854	0.1429	0.1429	0.2165	75 623 317
6	$\hat{m}\hat{m}b$	9838.313	15 270.315	6077.492	0.1429	0.1429	0.2098	77 249 778
7	$\hat{m}\hat{m}b$	9843.389	15 349.671	6088.822	0.1429	0.1429	0.2826	79 312 393
8	$\hat{m}b\hat{m}$	9839.985	15 408.858	6097.282	0.1429	0.2880	0.1429	80 866 069
9	$\hat{m}b\hat{m}$	9842.010	15 490.985	6109.011	0.1429	1.8422	0.1429	82 892 977
10	$\hat{m}b\hat{m}$	9839.964	15 548.367	6117.211	0.1429	0.4573	0.1429	**82 973 572**
11	$\hat{m}b\hat{m}$	9843.121	15 632.950	6129.287	0.1429	0.1720	0.1429	82 197 518
12	$\hat{f}b$	9853.493	15 501.562	6164.579	0.0638	0.7776	–	81 146 165
13	$\hat{f}b$	9857.259	15 525.142	6184.610	0.0358	0.8389	–	80 848 215
14	$\hat{f}b$	9863.145	15 500.162	6204.046	0.0062	0.7573	–	80 065 426
15	$\hat{f}b$	9861.849	15 521.812	6224.877	0.0250	0.9605	–	79 617 025

TABLE 5. Optimal labellings and the optimal location of the junction when the breakout point is at R_2.

Case	Optimal labelling	Optimal location of the junction			Gradients			Optimal NPV $
		x	y	z	g_1	g_2	g_3	
1	$\hat{m}\hat{m}b$	9806.628	15 087.881	6006.147	0.1429	0.1429	0.1968	71 646 672
2	$\hat{m}\hat{f}m$	10 446.32	15 508.587	6032.922	0.1429	0.1164	0.1429	71 126 748
3	$\hat{m}\hat{m}b$	9837.321	15 227.247	6026.125	0.1429	0.1429	0.2099	75 623 605
4	$\hat{m}\hat{m}b$	9832.052	15 288.990	6034.942	0.1429	0.1429	0.2174	77 426 363
5	$\hat{m}\hat{f}m$	10 206.75	15 524.947	6054.934	0.1429	0.0848	0.1429	76 909 490
6	$\hat{m}\hat{m}b$	9835.390	15 428.690	6054.902	0.1429	0.1429	0.3171	81 395 804
7	$\hat{m}\hat{m}b$	9842.118	15 508.049	6066.239	0.1429	0.1429	6.1140	**83 478 168**
8	$\hat{m}b\hat{m}$	9838.373	15 567.041	6074.668	0.1429	0.2633	0.1429	83 453 560
9	$\hat{m}b\hat{m}$	9841.598	15 649.195	6086.403	0.1429	0.1772	0.1429	82 747 849
10	$\hat{f}b$	9846.451	15 501.936	6123.909	0.0565	0.9591	–	82 080 387
11	$\hat{f}b$	9850.112	15 527.268	6144.418	0.0273	0.8013	–	81 774 692
12	$\hat{f}b$	9853.493	15 501.562	6164.579	0.0035	0.7776	–	81 102 771

https://doi.org/10.1017/S1446181120000231 Published online by Cambridge University Press

TABLE 6. Optimal labellings and the optimal location of the junction when the breakout point is at R_3.

Case	Optimal labelling	Optimal location of the junction			Gradients			Optimal NPV $
		x	y	z	g_1	g_2	g_3	
1	$\hat{m}\hat{m}b$	9814.879	15 237.789	5984.713	0.1429	0.1429	0.2258	75 097 182
2	$\hat{m}\hat{f}m$	10 263.88	15 520.726	6006.825	0.1429	0.1051	0.1429	74 772 343
3	$\hat{m}\hat{m}b$	9486.073	15 519.946	6012.988	0.1429	0.0852	0.1429	76 851 016
4	$\hat{m}\hat{m}b$	9833.128	15 439.177	6013.503	0.1429	0.1429	0.3470	81 145 107
5	$\hat{m}\hat{f}m$	9688.892	15 526.991	6023.865	0.1429	0.0032	0.1429	81 176 264
6	$\hat{m}\hat{m}b$	9834.175	15 578.459	6033.400	0.1429	0.1429	0.1799	**83 324 417**
7	$\hat{m}\hat{m}b$	9840.573	15 658.037	6044.758	0.1429	0.1429	0.1775	82 888 159
8	$\hat{f}b$	9841.863	15 504.792	6083.575	0.0536	0.9512	–	82 612 338
9	$\hat{f}b$	9840.487	15 521.042	6104.712	0.0231	1.2961	–	82 285 958
10	$\hat{f}b$	9846.451	15 501.936	6123.909	0.0056	0.9591	–	81 860 178

TABLE 7. Optimal labellings and the optimal location of the junction when the breakout point is at R_4.

Case	Optimal labelling	Optimal location of the junction			Gradients			Optimal NPV $
		x	y	z	g_1	g_2	g_3	
1	$\hat{m}\hat{m}b$	9819.311	15 378.169	5964.656	0.1429	0.1429	0.3092	78 537 061
2	$\hat{m}\hat{f}m$	10 072.77	15 528.310	5979.512	0.1429	0.0740	0.1429	78 511 903
3	$\hat{m}\hat{f}m$	9692.371	15 523.402	5983.521	0.1429	0.0018	0.1429	80 774 007
4	$\hat{m}\hat{m}b$	9830.962	15 579.285	5993.384	0.1429	0.1429	0.1843	**82 979 145**
5	$\hat{m}\hat{m}b$	9836.575	15 658.747	6004.720	0.1429	0.1429	0.1796	82 908 364
6	$\hat{f}b$	9842.123	15 511.853	6042.983	0.0535	0.2816	–	82 894 902
7	$\hat{f}b$	9838.533	15 525.413	6063.707	0.0227	0.1450	–	82 680 439
8	$\hat{f}f$	9824.143	16 174.721	6078.452	0.0076	0.0227	–	79 512 703

TABLE 8. Globally optimal solution.

Rubicon breakout	Hornet drawpoints	Optimal labelling	Optimal location of the junction			Gradients			Optimal NPV $
			x	y	z	g_1	g_2	g_3	
R_1	H_{10}, H_{11}	$\hat{m}b\hat{m}$	9839.964	15 548.367	6117.211	0.1429	0.4573	0.1429	82 973 572
R_2	H_7, H_8	$\hat{m}\hat{m}b$	9842.118	15 508.049	6066.239	0.1429	0.1429	6.1140	**83 478 168**
R_3	H_6, H_7	$\hat{m}\hat{m}b$	9834.175	15 578.459	6033.400	0.1429	0.1429	0.1799	83 324 417
R_4	H_4, H_5	$\hat{m}\hat{m}b$	9830.962	15 579.285	5993.384	0.1429	0.1429	0.1843	82 979 145

https://doi.org/10.1017/S1446181120000231 Published online by Cambridge University Press

Acknowledgements

The research was supported by Rand Mining and Tribune Resources. We would particularly like to thank Dr John Andrews, formerly of Rand Mining and Tribune Resources, for giving us the opportunity to work on a project with relevance to industry and for providing us with data for a case study. The financial support of an ARC Linkage Grant is gratefully acknowledged.

References

[1] E. Ben-Awuah, O. Richter, T. Elkington and Y. Pourrahimian, "Strategic mining options optimization: open pit mining, underground mining or both", *Int. J. Min. Sci. Technol.* **26** (2016) 1065–1071; doi:10.1016/j.ijmst.2016.09.015.

[2] M. Brazil, P. A. Grossman, D. H. Lee, J. H. Rubinstein, D. A. Thomas and N. C. Wormald, "Decline design in underground mines using constrained path optimization", *Min. Technol.* **117** (2008) 93–99; doi:10.1179/174328608X362668.

[3] M. Brazil, J. H. Rubinstein, D. A. Thomas, J. F. Weng and N. C. Wormald, "Gradient-constrained minimum networks (I). Fundamentals", *J. Glob. Optim.* **21** (2001) 139–155; doi:10.1023/A:1011903210297.

[4] M. Brazil and D. A. Thomas, "Network optimisation for the design of underground mines", *Networks* **49** (2007) 40–50; doi:10.1002/net.20140.

[5] M. Brazil, D. A. Thomas and J. F. Weng, "Gradient-constrained minimum networks (II). Labelled or locally minimal Steiner points", *J. Glob. Optim.* **42**(2008) 23–37; doi:10.1007/s10898-007-9201-x.

[6] M. Brazil and M. Zachariasen, *Optimal interconnection trees in the plane*, Volume 29 of *Algorithms Comb. Ser*. (Springer International Publishing, Cham, 2015); doi:10.1007/978-3-319-13915-9.

[7] K. Dagdelen, "Openpit optimization – Strategies for improving economics of mining projects through mine planning", *17th Int. Min. Congr. Exhib. of Turkey* (Chamber of Mining Engineers of Turkey, Ankara, Turkey, 2001) 117–121.

[8] P. A. Grossman, M. Brazil, J. H. Rubinstein and D. A. Thomas, "Scheduling the construction of value and discount weighted trees for maximum net present value", *Comput. Oper. Res.* **115** (2020) 104578; doi:10.1016/j.cor.2018.10.018.

[9] J. Hou, C. Xu, P. A. Dowd and G. Li, "Integrated optimisation of stope boundary and access layout for underground mining operations", *Min. Technol.* **128** (2019) 193–205; doi:25726668.2019.1603920.

[10] T. B. Johnson and R. W. Sharp, "A three dimensional dynamic programming method for optimal ultimate pit design", US Department of the Interior, Bureau of Mines, Report of Investigation 7553, Washington, 1971, available at https://books.google.com.au/books?id=XXu36F7yAasC&pg=PP1#v=onepage&q&f=false.

[11] B. King and A. Newman, "Optimizing the cutoff grade for an operational underground mine", *Interfaces* **48** (2018) 291–397; doi:10.1287/inte.2017.0934.

[12] H. Lerchs and I. F. Grossmann, "Optimum design of open pit mines", *Can. Inst. Min. Bull.* **58** (1965) 17–24.

[13] J. Little, E. Topal and P. Knights, "Simultaneous optimisation of stope layouts and long term production schedules", *Min. Technol.* **120** (2011) 129–136; doi:10.1179/1743286311Y.0000000011.

[14] M. Meyer, "Applying linear programming to the design of ultimate pit limits", *Manag. Sci.* **16** (1969) B121–B135, available at https://www.jstor.org/stable/2628495.

[15] A. M. Newman and M. Kuchta, "Using aggregation to optimize long-term production planning at an underground mine", *Eur. J. Oper. Res.* **176** (2007) 1205–1218; doi:10.1016/j.ejor.2005.09.008.

[16] A. M. Newman, E. Rubio, R. Caro, A. Weintraub and K. Eurek, "A review of operations research in mine planning", *Interfaces* **40** (2010) 222–245; doi:10.1287/inte.1090.0492.

[17] Northern Star Ltd (2015), Official website and factsheets, available at http://www.nsrltd.com/.
[18] K. G. Sirinanda, M. Brazil, P. A. Grossman, J. H. Rubinstein and D. A. Thomas, "Optimally locating a junction point for an underground mine to maximise the net present value", *ANZIAM J.* **55** (2014) C315–C328; doi:10.21914/anziamj.v55i0.7791.
[19] K. G. Sirinanda, M. Brazil, P. A. Grossman, J. H. Rubinstein, and D. A. Thomas, "Maximizing the net present value of a Steiner tree", *J. Glob. Optim.* **62** (2015) 391–407; doi:10.1007/s10898-014-0246-3.
[20] K. G. Sirinanda, M. Brazil, P. A. Grossman, J. H. Rubinstein and D. A. Thomas, "Time delayed discounted Steiner trees to locate two or more discounted Steiner points", *ANZIAM J.* **57** (2016) C253–C267; doi:10.21914/anziamj.v57i0.10400.
[21] K. G. Sirinanda, M. Brazil, P. A. Grossman, J. H. Rubinstein and D. A. Thomas, "Gradient-constrained discounted Steiner trees I – Optimal tree configurations", *J. Glob. Optim.* **64** (2016) 497–513; doi:10.1007/s10898-015-0326-z.
[22] K. G. Sirinanda, M. Brazil, P. A. Grossman, J. H. Rubinstein and D. A. Thomas, "Gradient-constrained discounted Steiner trees II – Optimally locating a discounted Steiner point", *J. Glob. Optim.* **64** (2016) 515–532; doi:10.1007/s10898-015-0325-0.
[23] K. G. Sirinanda, M. Brazil, P. A. Grossman, J. H. Rubinstein and D. A. Thomas, "Strategic underground mine access design to maximise the net present value", in: *Advances in Applied Strategic Mine Planning*, (Springer, Cham, 2018) 607–624; doi:10.1007/978-3-319-69320-0.
[24] L. P. Trout, "Underground mine production scheduling using mixed integer programming", *25th Int. APCOM Symp.*, Melbourne, Australia, (1995) 395–400, available at https://ausimm.com/product/underground-mine-production-scheduling-using-mixed-integer-programming/.
[25] Y. Zhao and Y. C. Kim, "A new graph theory algorithm for optimal ultimate design", *Proc. 23rd Int. APCOM Symp.*, (1992) 423–434, available at https://www.onemine.org/document/abstract.cfm?docid=173106&title=A-New-Graph-Theory-Algorithm-For-Optimal-Ultimate-Pit-Design.